Low-Loss and Compact V-Band MEMS-Based Analog Tunable Bandpass Filters

Hong-Teuk Kim, *Student Member, IEEE*, Jae-Hyoung Park, *Student Member, IEEE*, Yong-Kweon Kim, *Member, IEEE*, and Youngwoo Kwon, *Member, IEEE*

***Abstract*—This paper presents compact V-band MEMS-based analog tunable bandpass filters with improved tuning ranges and low losses. For compact size and wide tuning range, the two-pole filters are designed using the lumped-elements topology with metal–air–metal (MAM) bridge-type capacitors as tuning elements. Capacitive inter-resonator coupling has been employed to minimize the radiation loss, which is the main loss contributor at high frequencies. Two filters have been demonstrated at 50 and 65 GHz. The 65-GHz analog tunable filter showed a frequency tuning bandwidth of 10% (6.5 GHz) with low and flat insertion losses of 3.3 ± 0.2 dB over the entire tuning range.**

***Index Terms*—MEMS, tunable bandpass filter, V-band.**

I. Introduction

LOW-LOSS, compact tunable filters with micromachined varactors or switches can be effectively used for highly integrated multiband/multifrequency communication systems. Recently, a number of MEMS-based bandpass filters have demonstrated frequency tunability at microwave and millimeter-wave frequencies [1], [2]. Two different types of frequency tuning methods exist for MEMS-based filters, digital and analog. Only discrete center frequencies are possible for digital type while continuous frequencies are possible for the latter. Large frequency tuning range can be obtained from the digital MEMS filters, which use MEMS switches to turn on or off the resonating components, thereby changing the center frequencies. For example, 50% center frequency variation from 30 to 15 GHz was achieved by switching resonating components in [2].

MEMS analog tunable filters have been demonstrated for the first time by the authors at Ka-band [1]. The center frequency of these analog filters was tuned by changing the gap of the cantilever-based metal–air–metal (MAM) capacitors using electrostatic force. However, partial deflection of the cantilever beams and restricted deflection range before collapse limited the frequency tuning range. The resulting tuning range was limited to less than 4.2% with an insertion loss of about 4.5 dB near 30 GHz [1]. This rather high loss was attributed to the radiation loss from weak magnetic coupling between the spiral inductors and the dielectric loss coming from the lossy glass substrate in addition to the inevitable conductor losses.

The goal of this work is to develop MEMS-based analog tunable filters at higher frequencies (V-band) with lower losses and improved tuning ranges. The lumped-elements topology was employed together with bridge-type MAM capacitors for enhanced frequency tuning, and quartz substrate was used to reduce the substrate loss. In addition, capacitive coupling using MAM capacitors was used instead of weak magnetic coupling to reduce radiation losses at high frequencies.

II. Design and Fabrication

The V-band tunable filter design was optimized to achieve improved tuning range as well as reduced loss. As demonstrated in [1], tunable filters can be realized using two different topologies depending on the type of the resonators. Distributed-element type uses the transmission lines, while lumped-element type employs LC-based lumped elements, as the resonators. The resonating frequency is generally controlled by changing the gap of the MAM capacitors for MEMS-based analog tunable filters. For this purpose, the variable MAM capacitors are attached at the end of the transmission lines in distributed-element type while they are combined with fixed spiral inductors in lumped-element type tunable filters. Distributed-element type filters show smaller frequency tuning range compared with the lumped-element type since the effective capacitance variation of the resonators is reduced by the amount of the nonvariable capacitances inherent in the transmission lines. On the other hand, the tuning range of the lumped-elements filters is limited only by the variable capacitance range of the MAM capacitors without any nonvariable offsets. Considering that a maximum gap control range of typical MAM capacitors is around 2/3 of the initial gap [3], the maximum frequency shift is estimated to be about 13.4% for lumped-elements type filters.

In this work, lumped-elements type resonators were used to achieve wider tuning range. Fig. 1 shows schematic and equivalent circuit schematic of the two-pole tunable bandpass filters. MAM capacitors were implemented using bridge-type beams rather than the cantilever types as in [1] since they are more stable and less sensitive to bending problems. The variable capacitance range is also slightly larger in bridge types due to the lack of unbalanced deflection. Bridge-type beams have been successfully demonstrated in low-loss MEMS phase shifters [4], [5].

The insertion loss of the V-band filter is improved by minimizing the radiation loss, which becomes a major loss contributor at high frequencies. In order to reduce the radiation loss,

Manuscript received March 4, 2002; revised May 29, 2002. This work was supported by the Korean Ministry of Science and Technology through the Creative Research Initiative Program. The review of this letter was arranged by Associate Editor Dr. Arvind Sharma.

The authors are with the Center for 3-D Millimeter-Wave Integrated Systems, School of Electrical Engineering, Seoul National University, Seoul, Korea (e-mail: htkim@snu.ac.kr; ykwon@snu.ac.kr).

Digital Object Identifier 10.1109/LMWC.2002.805543

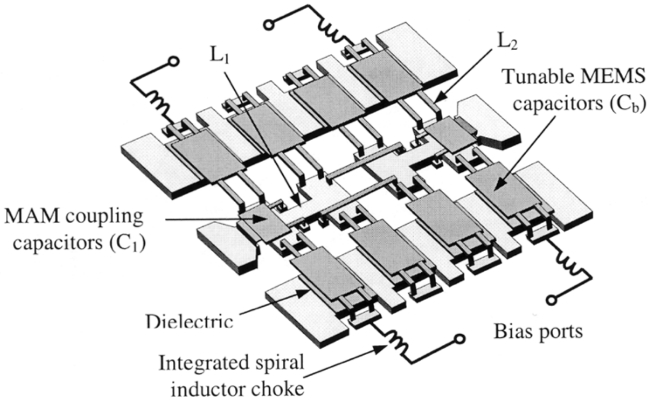

(a)

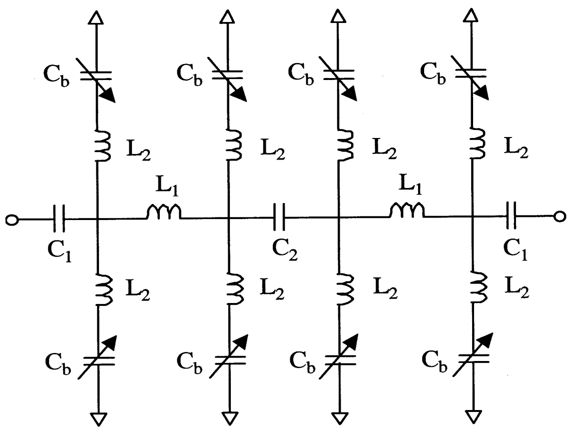

(b)

Fig. 1. (a) Schematic and (b) the equivalent circuit of the MEMS tunable bandpass filter.

capacitive coupling using MAM capacitors, instead of magnetic coupling, has been employed between the resonators. The electric field is confined in the air between the overlapped conductor plates in MAM structures, resulting in reduced radiation loss as well as substrate loss. MAM capacitors were also used between the resonators and the ports.

The filters are initially designed based on the lumped-element equivalent circuit shown in Fig. 1(b). Two filters were designed at two different frequencies, 50 and 65 GHz. The detailed parameter values are listed in Table I. Inductors and capacitors were implemented using high-impedance CPW lines and MAM capacitors, respectively. The initial dimensions of MAM structures were calculated analytically, ignoring the fringing field. Next, a commercial electromagnetic (EM) software, IE3D, is used for the full wave analysis of the filter, during which the dimensions of the lumped elements in the resonators and the coupling capacitors are tuned until the desired filter characteristics are achieved.

The filters were fabricated with electroplated gold structures on a 520-μm-thick quartz substrate ($\varepsilon_r = 3.8$). The thickness of the CPW line and the bridge is 3 μm and 2 μm, respectively. A 0.3-μm-thick silicon nitride was deposited with plasma enhanced chemical vapor deposition (PECVD) over the CPW ground plane under the bridges to avoid dc short. The details of the fabrication techniques have been reported in [5]. The air gap is 1.1 μm. The top plate sizes of MEMS capacitors for

TABLE I
LUMPED ELEMENTS PARAMETERS OF THE FILTERS. C_{b0} IS ZERO-BIAS (0 V) CAPACITANCE OF MEMS BRIDGE CAPACITOR (C_b) IN FIG. 1(a)

Type	C_1 (fF)	C_2 (fF)	L_1 (pH)	L_2 (pH)	C_{b0} (fF)
50-GHz Filter	78	46	80	11	86
65-GHz Filter	66	42	56	10	74

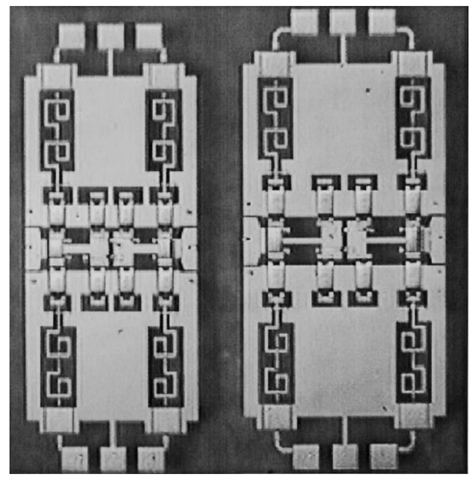

Fig. 2. Photographs of the fabricated V-band tunable filters.

50- and 65-GHz filters are 62 $\times$ 112 μm and 60 $\times$ 100 μm, respectively. The dimensions of center CPW lines used as inductors (L_1) are width $= 25$ μm/35 μm, gap $= 92$ μm/77 μm, and length $= 150$ μm/98 μm for 50-/65-GHz filters, respectively. L_2 represents the inductance of MEMS bridge with two narrow parallel beams (width $= 20$ μm, length $= 40$ μm). Fig. 2 shows the fabricated tunable filters. DC bias voltage is applied between the movable bridge capacitors and a common CPW top ground plate through the integrated spiral inductor chokes and shunt MIM capacitors. Total inductance of the two-cascaded spiral inductor is 0.7 nH with self-resonance frequency higher than 87 GHz. The bias circuit is provided symmetrically on both sides of the circuits. The chip sizes are 780 μm $\times$ 1970 μm and 670 μm $\times$ 1900 μm for 50- and 65-GHz filters, respectively.

III. MEASUREMENTS

Fig. 3 shows the measured and simulated filter responses at zero bias voltage. Aside from a little discrepancy in the insertion loss and center frequency, the results are generally in good agreement. The measured center frequencies are 51.7 GHz with 1-dB bandwidth of 8.5%, and 65.5 GHz with 1-dB bandwidth of 10.5%. The total insertion losses are 2.65 dB and 3.1 dB for 50- and 65-GHz filters, respectively. The loss due to the bias circuits is estimated to be about 0.8 dB from the measured data as well as the EM simulation that includes the effect of the integrated spiral inductors. Measured bias tuning characteristics of the two filters are shown in Fig. 4. The bias was increased gradually while considering the pull-in voltages of the bridge

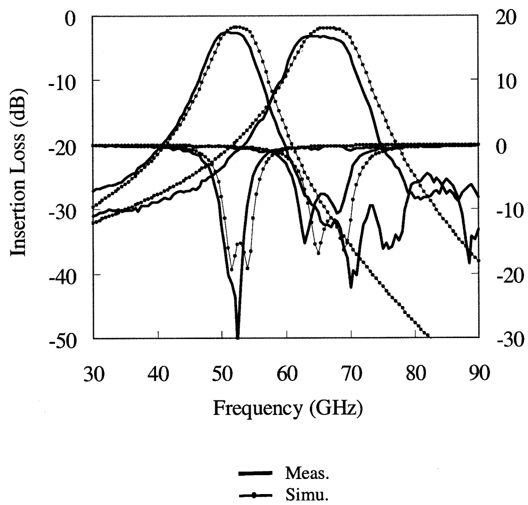

Fig. 3. Measured and simulated filter responses at zero bias voltage.

capacitors, which were between 22 and 25 V. The center frequencies of the two filters varied as much as 4.2 GHz (8.1%) from 51.7 to 47.5 GHz, and 6.5 GHz (10.0%) from 65.5 to 59 GHz. The 1-dB bandwidths also changed slightly during frequency tuning; the bandwidth for the 50-GHz filter decreased from 8.5% (51.7 GHz) to 6.4% at 47.5 GHz, and that for 65-GHz filter decreased from 10.5% (65.5 GHz) to 7.6% at 59 GHz. From these results and the simulations using the equivalent circuit model of Fig. 1(b), the corresponding capacitance variations of MAM capacitors were extracted and were estimated to be more than 20%. These capacitance tuning ranges are reasonable for analog mode of operation, considering the deflection limit of the bridge structures before collapse [3], [4]. It is worthwhile to note from Fig. 4 that the insertion losses at the center frequencies did not change appreciably throughout the entire tuning ranges; the insertion losses are within 3.0 ± 0.45, and 3.3 ± 0.2 dB. Compared with the previous work [1], these results show lower loss and wider frequency tuning at even higher frequency band. This is mainly attributed to the capacitive inter-resonator coupling, and the use of the lumped-element approach using low-loss MAM capacitors as varactors.

IV. Conclusion

V-band analog tunable filters using micromachined variable capacitors have been designed and fabricated using MEMS technology. The combined effects of the lumped-elements type topology using MAM capacitors and the capacitive coupling between the resonators resulted in the improved frequency tuning range (10.0% at 65.5 GHz) together with the reduced insertion loss (3.3 ± 0.2 dB) when compared with our previous work at Ka-band [1]. These low-loss and compact tunable MEMS filters can be effectively used for highly integrated multiband/multifrequency millimeter-wave systems at V-band and above.

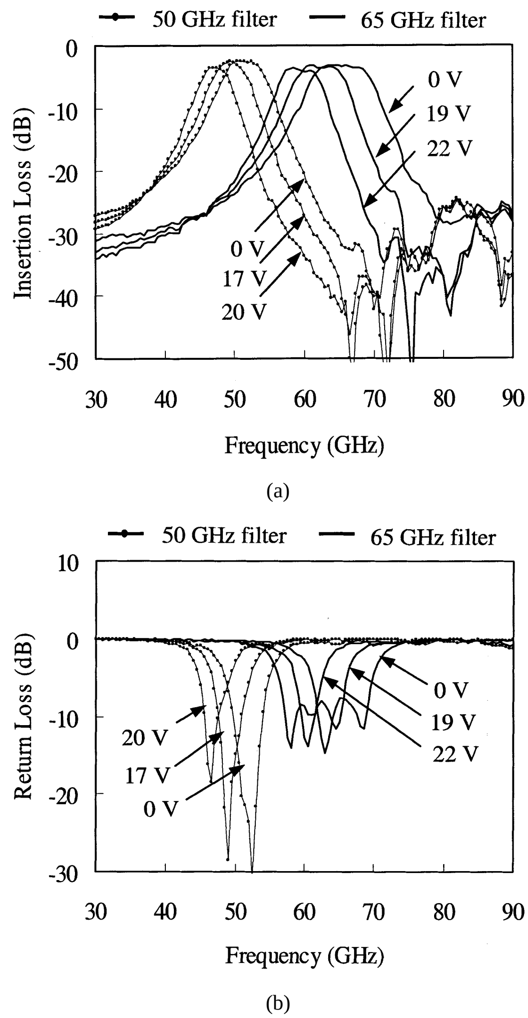

Fig. 4. Measured (a) insertion losses and (b) return losses of the tunable filters for various bias voltages. The second bias voltages (17 and 19 V) correspond to the voltages required to tune the filters to the middle of the entire tuning range.

References

[1] H. T. Kim, J. H. Park, Y. K. Kim, and Y. Kwon, “Millimeter-wave micromachined tunable filters,” in *IEEE MTT-S Dig.*, vol. 3, June 1999, pp. 1235–1238.

[2] D. Peroulis, S. Pacheco, K. Sarabandi, and L. P. B. Katehi, “Tunable lumped components with applications to reconfigurable MEMS filters,” in *IEEE MTT-S Dig.*, May 2001, pp. 341–344.

[3] C. Goldsmith, J. Randall, S. Eshelman, T. H. Lin, D. Denniston, S. Chen, and B. Norvell, “Characteristics of micromachined switches at microwave frequencies,” in *IEEE MTT-S Dig.*, Jun. 1995, pp. 1141–1144.

[4] N. S. Barker and G. M. Rebeiz, “Distributed MEMS true-time delay phase shifters and wideband switches,” *IEEE Trans. Microwave Theory Tech.*, vol. 46, pp. 1881–1890, Nov. 1998.

[5] J. H. Park, H. T. Kim, K. Kang, Y. Kwon, and Y. K. Kim, “A micromachined milleter wave phase shifter using semi-lumped elements,” in *11th Int. Conf. Solid-State Sens. Actuators Transducers*, 2001, pp. 1552–1555.